

Received: 2020.01.31

Accepted: 2020.03.01

Available online: 2020.05.22

Published: 2020.07.18

# Lipopolysaccharide-Induced Acute Lung Injury Is Associated with Increased Ran-Binding Protein in Microtubule-Organizing Center (RanBPM) Molecule Expression and Mitochondria-Mediated Apoptosis Signaling Pathway in a Mouse Model

Authors' Contribution:

Study Design A  
Data Collection B  
Statistical Analysis C  
Data Interpretation D  
Manuscript Preparation E  
Literature Search F  
Funds Collection G

BCDEF 1,2 **Xiaojing Lv\***  
BCDEF 1,2 **Xiaomin Lu\***  
ABDEG 1,2 **Jiping Zhu**  
BCF 1,2 **Qian Wang**

1 Jiangsu Province Hospital of Chinese Medicine, Nanjing, Jiangsu, P.R.China  
2 Affiliated Hospital of Nanjing University of Chinese Medicine, Nanjing, Jiangsu, P.R.China

\* Xiaojing Lv and Xiaomin Lu contributed equally to this study

**Corresponding Author:** Jiping Zhu, e-mail: zzz-one@163.com

**Source of support:** This study was funded by the National Natural Science Foundation of China (Grant No. 81774081)

**Background:** Acute lung injury (ALI) is a severe and life-threatening disorder treated in intensive care units. This study aimed to determine molecules or associated signaling pathways that are involved in lipopolysaccharide (LPS)-induced inflammation in an ALI model.

**Material/Methods:** An ALI mouse model was established by administering LPS (25 mg/kg via intratracheal instillation). Thirty-two ALI mice were divided into Model-4 h, Model-8 h, Model-12 h, and Model-24 h groups, while another 8 mice without LPS treatment were assigned as the Control group. Hematoxylin-eosin (HE) staining was used to evaluate inflammation of lung tissues. Wet weight/dry weight (W/D) ratio and myeloperoxidase (MPO) activity of lung tissue in ALI mice were evaluated. Expressions of Bcl-2, Bcl-XL, Bak, Bax, cleaved caspase-3 (C-caspase-3), and Ran-binding protein in microtubule-organizing center (RanBPM) were determined using Western blot analysis.

**Results:** LPS administration caused obvious inflammatory cell infiltration of lung tissues in ALI mice. The W/D ratio of ALI mouse lung tissues was significantly higher in Model groups than in the Control group ( $p < 0.05$ ). MPO activity of ALI mice was remarkably higher in Model groups compared to the Control group ( $p < 0.05$ ). LPS-induced ALI model mice exhibited significantly higher levels of C-caspase 3 lung tissues compared to the Control group ( $p < 0.05$ ). LPS-induced ALI model mice had significantly lower Bcl-XL/Bcl-2 and remarkably higher Bak/Bax expression compared with the Control group ( $p < 0.05$ ). LPS-induced ALI model mice displayed obviously higher RanBPM expression than in the Control group ( $p < 0.05$ ).

**Conclusions:** Lipopolysaccharide-induced acute lung injury is associated with increased RanBPM molecule expression and with mitochondria-mediated apoptosis signaling pathway in a mouse model.

**MeSH Keywords:** **Acute Lung Injury • Apoptosis • Inflammation • Lipopolysaccharides**

**Full-text PDF:** <https://www.medscimonit.com/abstract/index/idArt/923172>

 2561   7  34



## Background

Acute lung injury (ALI) is a severe and life-threatening disorder that usually occurs in intensive care units (ICU) worldwide [1,2]. ALI is generally induced by respiratory infections, inhalation damage, gastric-contents aspiration, trauma, and sepsis [3]. ALI occurs appropriately in 2 000 000 individuals each year worldwide, causing high rates of mortality and morbidity [4]. Clinically, ALI is mainly characterized by pulmonary edema, alveolar infiltration, and diffuse inflammation [5]. Although the clinical symptoms are usually similar, the underlying triggers for ALI can be heterogeneous, such as acute respiratory distress syndrome [6] and blood transfusions in transfusion-related acute lung injury (TRALI) [7]. In murine TRALI models, LPS has been used as a priming agent [8,9]. The high mortality rates of ALI patients are partly due to lack of understanding of the specific mechanisms underlying the pathogenesis and lack of effective treatments.

The increased alveolar capillary membrane permeability participates in the pathophysiological mechanism of ALI and is caused by intensive inflammation [10], leading to clinical manifestations such as severe hypoxemia, poor lung compliance, and serious bilateral infiltration. Endotoxin inhalation in animals can be used to mimic ALI caused by gram-negative bacteria, inducing pulmonary edema, neutrophil recruitment, and gas exchange damage [11]. Myeloperoxidase (MPO) can catalyze formation of oxidants and reflects the infiltration of neutrophils [12]. The wet weight/dry weight (W/D) ratio can reflect the degree of pulmonary edema in lung tissues [13]. Therefore, MPO and W/D ratio are considered to be markers for ALI pathology.

In recent years, a lipopolysaccharide (LPS)-induced approach has been extensively used as an efficient strategy for generating an ALI animal model by triggering inflammatory responses [14,15]. LPS is usually administered by inhalation, with a dose of 25 mg/kg for mice [15]. The LPS-induced ALI animal model has become a widely acknowledged strategy for exploring anti-ALI drugs and studying potential mechanisms. Although many studies have assessed pathogenetic factors for ALI, the mortality rate has remained relatively unchanged [16], and the molecular signaling pathway involved in LPS-caused ALI in the mouse model is unclear.

There are many signaling pathways involved in apoptosis, and it has been reported that the mitochondria-mediated apoptotic signaling pathway is involved in ALI [17]. The mitochondria-mediated apoptotic pathway involves anti-apoptotic molecules (Bcl-XL and Bcl-2) and pro-apoptotic molecules (Bax and Bak), which are biomarkers for mitochondria-mediated apoptosis [18]. Ran-binding protein in microtubule-organizing center (RanBPM) acts as an acetylcholinesterase-interacting molecule

and participates in apoptosis [19]. Therefore, we speculated that the mitochondria-mediated apoptotic signaling pathway and the RanBPM molecule participate in ALI pathogenesis.

In the present research, the LPS-caused ALI mouse model was generated and demonstrated severe inflammatory responses. The inflammation was observed *in vivo* and the apoptosis-associated molecules or signaling pathways involved in acute lung injury were explored in this study. Our results may provide an effective basis for assessing acute lung injury through targeting the mitochondria-mediated apoptosis signaling pathway and RanBPM in future investigations.

## Material and Methods

### Establishment of the ALI animal model

The C57BL/6 mice, age 6–8 weeks and weight 200–220 g, were obtained from the Experimental Animal Center of Nanjing University of Traditional Chinese Medicine. The mice had free access to standard diet and water. The acute lung injury mouse model was established according to the method previously published [20,21], with some modifications. Briefly, the ALI mouse model was established via nasal administration of 25 mg/kg LPS (Sigma-Aldrich, St. Louis, MO, USA).

The animal experiments were conducted according to the 1996 NIH Guidelines for Care and Use of Laboratory Animals. This study was approved by the Institutional Animal Care and Use Committee (IACUC) of Nanjing University of Traditional Chinese Medicine.

### Trial grouping and sample collection

We randomly assigned 40 mice into a 5 groups: the Control group (administering with PBS, n=8), the Model-4 h group (administered 25 mg/kg LPS by intratracheal instillation and killed 4 h after administration), the Model-8 h group (administered LPS 25 mg/kg by intratracheal instillation and killed 8 h after administration), the Model-12 h group (administered LPS 25 mg/kg by intratracheal instillation and killed 12 h after administration), and the Model-24 h group (administered 25 mg/kg LPS by intratracheal instillation and killed 24 h after administration). In ALI model groups, the dosage of LPS (25 mg/kg) was administered to mice according to the method described in a previous study [22]. Mice in each group were killed at different time points and lung tissues were isolated for experiments.

## Hematoxylin-eosin (HE) staining

The isolated lung tissues of mice were fixed using 10% buffered formalin (Sigma-Aldrich) for 24 h and dehydrated via washing with gradient ethanol (Sigma-Aldrich). Lung tissues were then embedded in paraffin and cut into 5- $\mu$ m sections for HE staining. Images of stained sections were obtained by fluorescence microscopy (model X71, Olympus, Tokyo, Japan) by randomly selecting 20 fields. The HE-stained histological images were scored using a histological scoring system described in a previous study [23], using the formula:  $\text{Score} = [(20 \times A) + (14 \times B) + (7 \times C) + (7 \times D) + (2 \times E)] / (\text{number of fields} \times 100)$ , in which A represents neutrophils in alveolar space, B represents neutrophils in interstitial space, C represents hyaline membranes, D represents proteinaceous debris-filling airspaces, and E represents alveolar septal thickening.

## Evaluation for wet weight/dry weight (W/D) ratio for lung tissue

At 4 h, 8 h, 12 h, and 24 h after administration of LPS, mice were killed and lung tissues were isolated. The freshly harvested lung tissue was weighed using an electronic balance and defined as the wet weight of lung tissue. Then, the lung tissues were dried in an oven at 80°C for 48 h, achieving the constant weight of tissues (weight difference between 2 consecutive times was less than 0.3 mg). Finally, we calculated the ratio of wet weight to dry weight (W/D ratio).

## Myeloperoxidase (MPO) activity assay

The MPO activity of lung tissue was measured using the MPO Detection Kit (Cat. No. A044, Nanjing Jiancheng Bioengineering Institute, Nanjing, China), according to the protocol of the manufacturer.

## Western blot assay

The lung tissues of mice were pooled together and lysed using RIPA lysis buffer (Beyotime Biotech, Shanghai, China) to obtain the proteins, which were then quantified, loaded onto SDS-PAGE gels, and electro-transferred onto PVDF membranes (Amersham Biosciences, Piscataway, NJ, USA). PVDF membranes were blocked with 5% non-fat milk and then incubated with rabbit anti-human Bcl-XL (Cat. No. ab32370, 1: 3000), rabbit anti-human Bcl-2 (Cat. No. ab32124, 1: 3000), rabbit anti-human Bak (Cat. No. ab32371, 1: 2000), rabbit anti-human Bax (Cat. No. ab182733, 1: 2000), rabbit anti-human RanBPM (Cat. No. ab205954, 1: 2000), rabbit anti-cleaved caspase-3 (Cat. No. ab2302, 1: 2000), and rabbit anti-human  $\beta$ -actin (Cat. No. ab1376, 1: 2000) overnight at 4°C. Subsequently, PVDF membranes were washed in phosphate-buffered saline Tween-20 (PBST, Beyotime Biotech) and incubated using

HRP-labeled goat anti-rabbit IgG (Cat. No. ab6721, 1: 1000) for 2 h at room temperature. Western blotting bands were visualized with a BeyoECL kit (Cat. No. P0018S, Beyotime Biotech). Finally, stained images were analyzed with the Tanon 5200 Automatic Chemiluminescence Imaging Analysis System (Tanon Sci. Tech. Co., Shanghai, China).

## Statistical analysis

Data are shown as mean  $\pm$  standard deviation (SD) and were analyzed using professional SPSS software (version: 22.0, SPSS, Inc., Chicago, IL, USA). Tukey's post hoc test validated ANOVA was used to compare the data among multiple groups. A *p* value less than 0.05 was defined as indicating a statistically significant difference.

## Results

### Histopathological evaluation for lung tissues

In the Control group, the alveolar structure was normal, the alveolar wall was thin, and there was no inflammatory cell infiltration in the alveolar cavity (Figure 1A). Model-4 h, Model-8 h, Model-12 h, and Model-24 h groups had pulmonary capillary congestion, pulmonary hemorrhage, neutrophil aggregation or infiltration in the pulmonary space of the vascular wall, and thickening of the alveolar wall or formation of a transparent membrane (Figure 1A). The pathology of lung tissues was the most significant in the Model-24 h group (Figure 1A). The statistical analysis of histological scores showed that the Model groups had significantly higher histological scores compared to the Control group (Figure 1B, *p*<0.05), especially for the Model-24 h group, which had the highest histological score among all Model groups (Figure 1B).

### W/D ratio was increased in lung tissues of ALI mice

Compared to the Control group, W/D ratios of Model groups were significantly increased (Figure 2, *p*<0.05). Compared with the Model-8 h group and Model-24 h group, the W/D ratio of the Model-4 h group was also remarkably increased (Figure 2, *p*<0.05). However, no significant differences were found among the Model-8 h, Model-12 h, and Model-24 h groups (Figure 2, *p*>0.05).

### MPO activity was increased in lung tissues for ALI mice

The results indicated that MPO activities for Model groups were significantly higher than in the Control group (Figure 3, *p*<0.05). Moreover, no significant differences were discovered in MPO activity among all 4 Model groups (Figure 3, *p*>0.05).

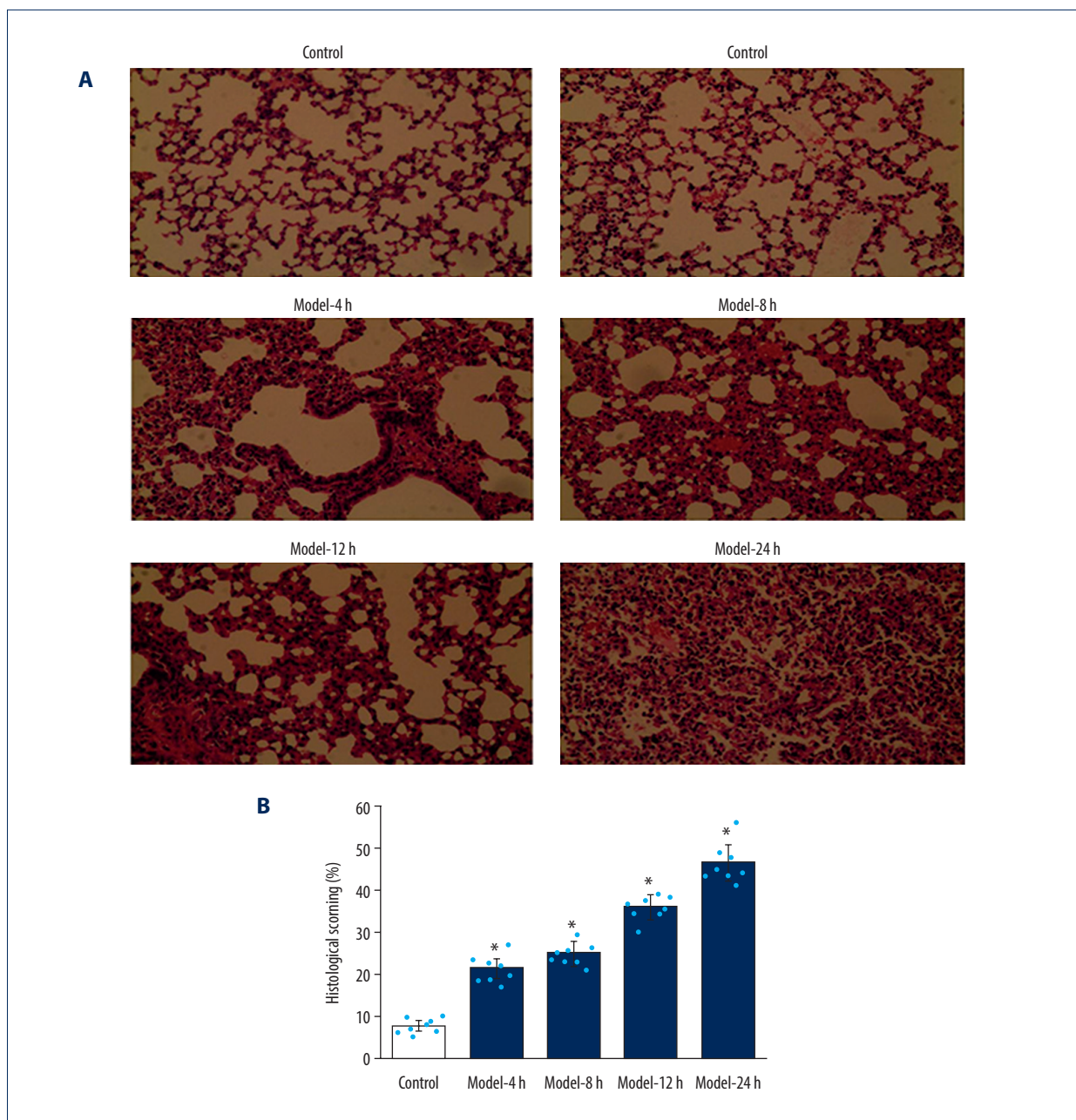


**Figure 1.** Pathological changes of inflammations in lung tissues for the ALI mouse models in different groups according to HE staining. **(A)** HE staining images. **(B)** Statistical analysis of histological scores for HE-stained images. Magnification, 100 $\times$ . \*  $p < 0.05$  vs. Control group.

### LPS-induced ALI model mice exhibited high levels of cleaved caspase 3 in lung tissues

According to the results of Western blot assay for assessing cleaved caspase 3 (C-caspase 3) expression (Figure 4A), we found that the C-caspase 3 expression was significantly higher in the Model-8 h, Model-12 h, and Model-24 h groups than in the Control group (Figure 4B,  $p < 0.05$ ). Additionally, C-caspase 3 expression was also remarkably higher in the Model-24 h

group compared to that in the Model-4 h, Model-8 h, and Model-12 h groups (Figure 4B,  $p < 0.05$ ).

### LPS-induced ALI model illustrated decreased anti-apoptotic molecules expression

In this study, the levels of anti-apoptotic molecules Bcl-XL and Bcl-2 were assessed using Western blot assay (Figure 5A), showing that expression of Bcl-XL molecule was remarkably lower

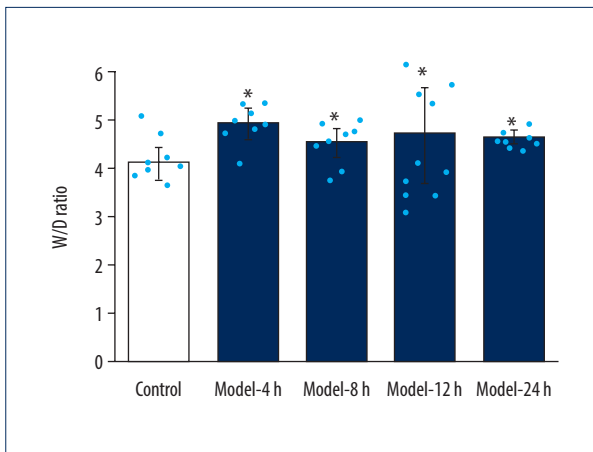


**Figure 2.** Determination for W/D ratio of the lung tissues in ALI mice of different groups. \*  $p < 0.05$  vs. Control group.

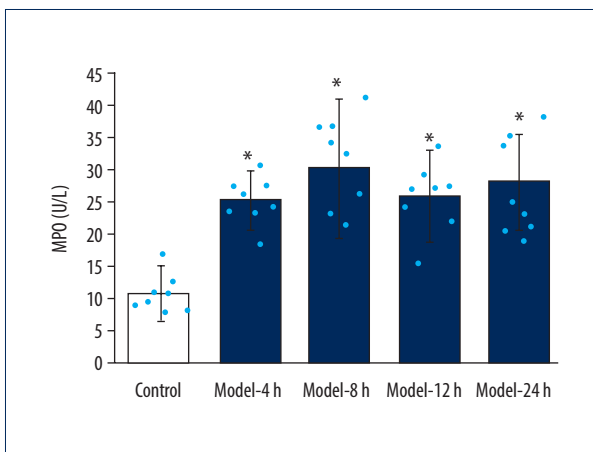


**Figure 3.** MPO activity evaluation of lung tissues for ALI mouse models in different groups. \*  $p < 0.05$  vs Control group.

in the Model groups compared with that of the Control group (Figure 5B,  $p < 0.05$ ), but no significant differences were found in expression of Bcl-XL molecule among the Model groups (Figure 5B,  $p > 0.05$ ). Moreover, Bcl-2 expression in Model groups was also remarkably lower compared to that of the Control group (Figure 5C,  $p < 0.05$ ). Also, expression of Bcl-2 molecule of Model-24 h group was remarkably lower compared to that of the Model-4 h and Model-8 h groups (Figure 5C,  $p < 0.05$ ). Additionally, after treatment with LPS, Bcl-2 expression demonstrated a time-dependent increase (Figure 5C).

### LPS-induced ALI model demonstrated increased pro-apoptotic molecules expression

We also assessed the expression of the pro-apoptotic molecules Bak and Bax using Western blot assay (Figure 6A). Our findings demonstrated that expression of Bak molecule in Model groups was obviously higher than in the Control group (Figure 6B,  $p < 0.05$ ). Expression of Bax molecule of in the Model groups

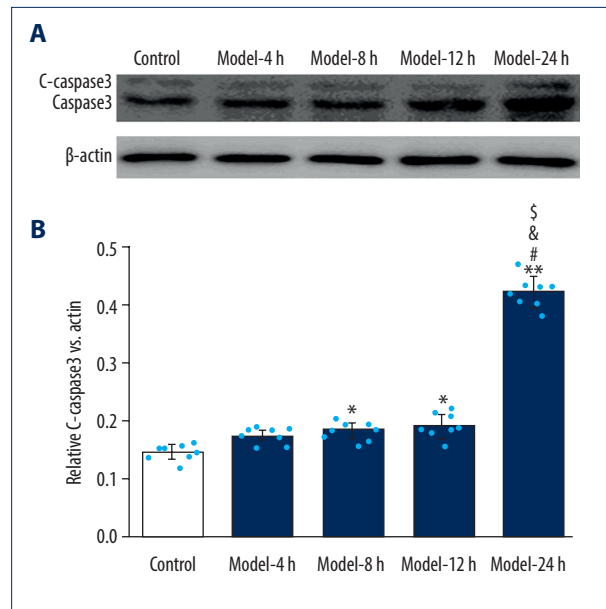


**Figure 4.** Effects for the LPS administration on C-caspase 3 expression in the lung tissues of the ALI mouse models. (A) Western blotting images for expressed C-caspase 3. (B) Statistical analysis for expression of C-caspase 3 in lung tissues of mice. The lung tissues of mice in each group were pooled together for Western blotting assay. \*  $p < 0.05$  vs. Control group; #  $p < 0.05$  vs. Model-4 h group; §  $p < 0.05$  vs. Model-8 h group; &  $p < 0.05$  vs. Model-12 h group.

was remarkably higher than in the Control group (Figure 6C,  $p < 0.05$ ), but we found no significant differences in Bak and Bax expression among all Model groups (Figure 6B, 6C,  $p > 0.05$ ).

### LPS-induced ALI model displayed enhanced RanBPM expression in lung tissues

In this study, we also verified expression of Ran-binding protein in microtubule-organizing center (RanBPM) using Western blot assay (Figure 7A). The present results showed that expression of RanBPM was obviously higher in Model groups compared with the Control group (Figure 7B,  $p < 0.05$ ). Moreover, expression of RanBPM molecule was remarkably higher in the Model-24 h group compared to that in the Model-4 h, Model-8 h, and Model-12 h groups (Figure 7B,  $p < 0.05$ ).

## Discussion

ALI is a critical clinical disorder caused by internal and external factors, with typical clinical manifestations of progressive dyspnea and refractory hypoxemia [24,25]. The specific mechanism underlying ALI is unknown and there is no effective treatment. The ALI model induced by LPS is closely related to the pathological injury of pneumonia, which is characterized by release

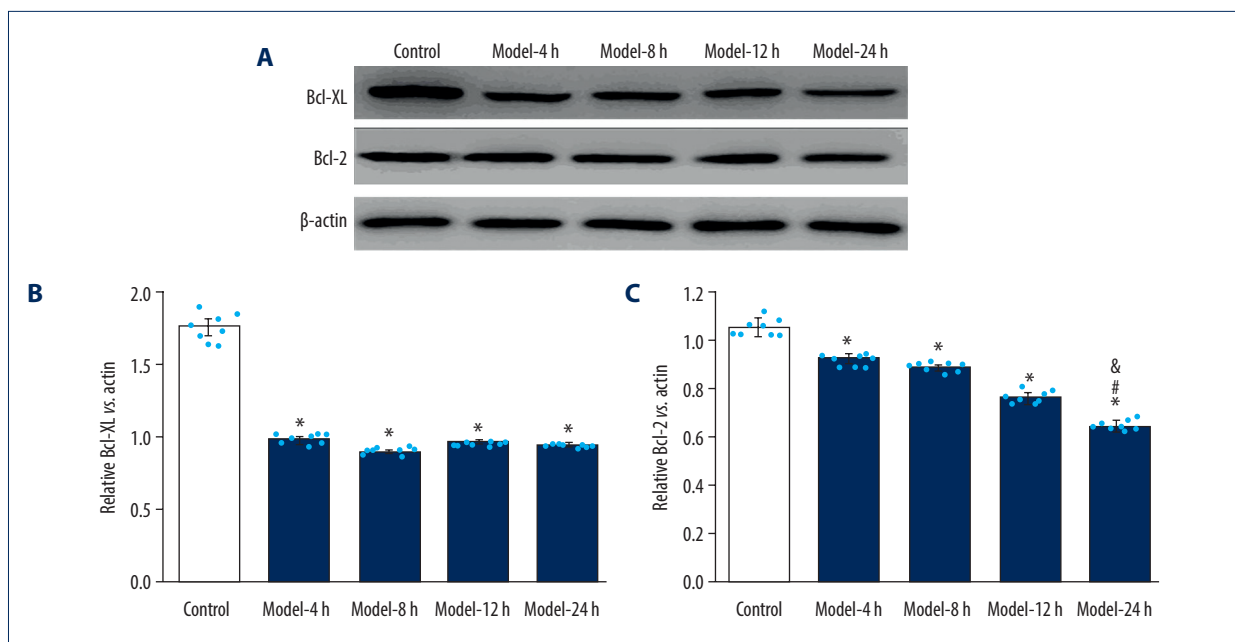


**Figure 5.** Evaluation for effects of LPS administration on Bcl-XL and Bcl-2 expression in lung tissues for ALI mouse models. **(A)** Western blotting images for expression of the Bcl-XL and Bcl-2. **(B)** The statistical analysis of the expression of Bcl-XL molecule in the lung tissues. **(C)** Statistical analysis for expression of Bcl-2 molecule in lung tissues of mice. The lung tissues of mice in each group were pooled together for Western blotting assay. \*  $p < 0.05$  vs. Control group; <sup>#</sup>  $p < 0.05$  vs. Model-4 h group; <sup>&</sup>  $p < 0.05$  vs. Model-8 h group; <sup>§</sup>  $p < 0.05$  vs. Model-12 h group.

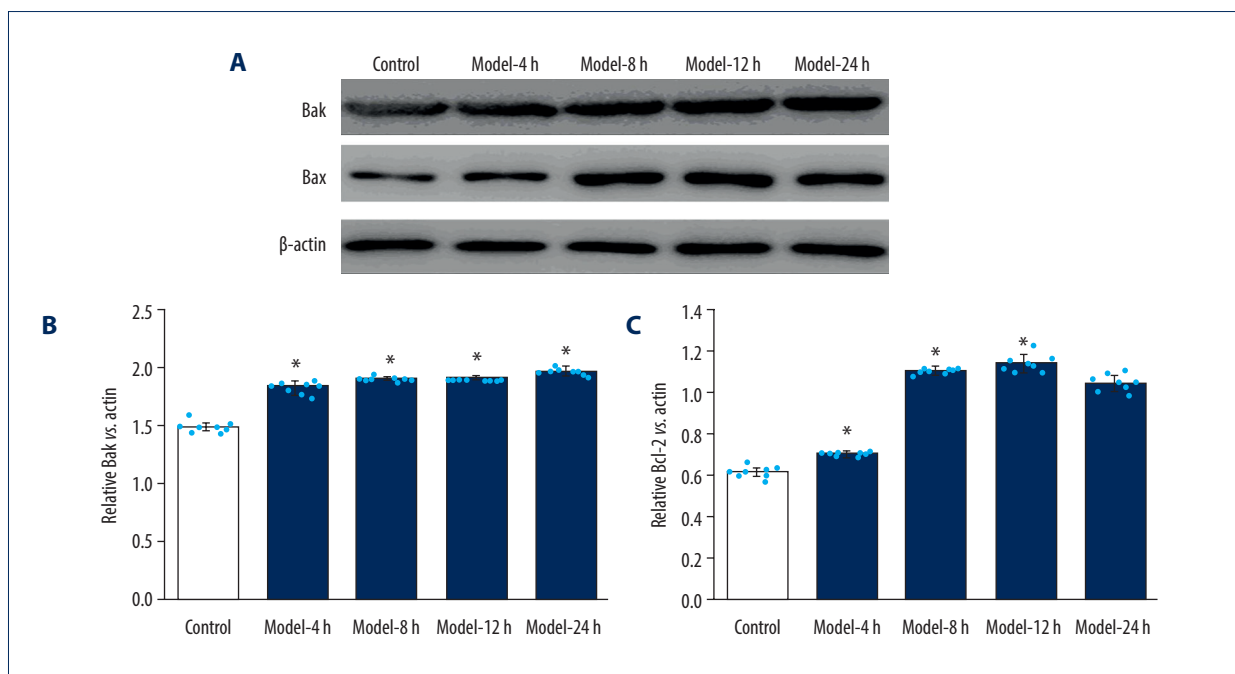


**Figure 6.** LPS administration reduced expression of Bak and Bax in lung tissues for the ALI mouse models. **(A)** Western blotting images for expression of the Bak and Bax molecules. **(B)** The statistical analysis of expression of Bak molecule in lung tissues of mice. **(C)** Statistical analysis of expression of Bax molecule in lung tissues of mice. The lung tissues of mice in each group were pooled together for Western blotting assay. \*  $p < 0.05$  vs. Control group.

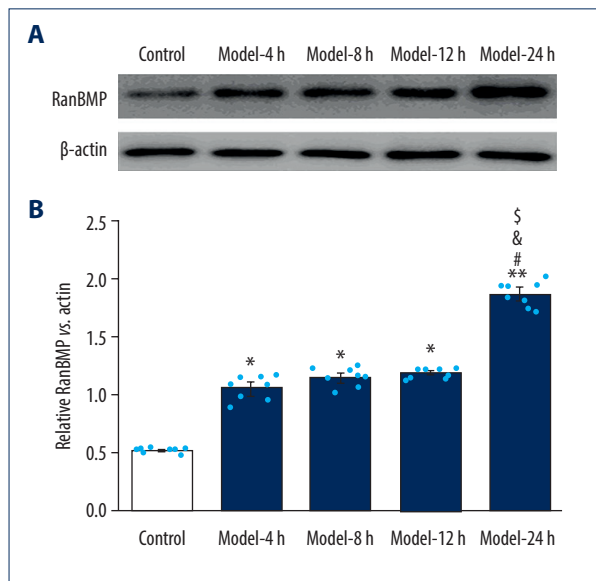


**Figure 7.** LPS-induced ALI mice demonstrated higher RanBPM expression in the lung tissues of the ALI mouse models. **(A)** Expression of RanBPM molecule determined using Western blotting. **(B)** The statistical analysis of the expression of RanBPM molecule in lung tissues of mice. The lung tissues of mice in each group were pooled together for Western blotting assay. \*  $p < 0.05$  vs. Control group.

of a many inflammatory mediators and infiltration of neutrophils in lung tissues [26]. In the present study, the pathological manifestations of lung tissues in an LPS-caused ALI mouse model were congestion, hemorrhage, and microthrombosis of pulmonary microvasculature. The presence of abundant edema fluid and inflammatory cell infiltration in pulmonary interstitium and alveoli shows that the ALI mouse model was successfully generated by treatment with LPS.

The main reasons for increased wet weight of lung tissue are pulmonary interstitial and alveolar edema, increased inflammatory cells, protein exudation, vascular congestion, and thrombosis [27]. The main reasons for the increase of dry weight are protein exudation, thrombosis, and increased numbers of inflammatory cells [27]. The W/D ratio of lung tissue is considered an important index to reflect degree of pulmonary edema [13]. MPO, a peroxidase released by neutrophils, can reflect the activation and infiltration of neutrophils [12]. Compared with the Control group, the W/D ratio and MPO activity in lung tissues of the Model groups were significantly higher, which suggests that the LPS-induced ALI mouse model was successfully established. The significant increase of W/D ratio in the Model-4 h group might be associated with the early inflammatory edema of lung tissues of ALI mice.

The regulatory pathways of apoptosis include mitochondria-mediated pathway, death receptor-mediated pathway, and endoplasmic reticulum-mediated pathway, and the mitochondria-mediated pathway is attracting growing attention [28]. In the mitochondria-mediated pathway, the pro-apoptotic BH3 molecule is activated by the toxic stimulation and interacts with anti-apoptotic Bcl-2 or Bcl-xL by inhibiting Bcl-2 or Bcl-xL expression [29]. Bax and Bak can freely induce mitochondrial permeability to increase and release cytochrome C, then activate caspase 9 and further activates caspase 3, and finally induce apoptosis [30]. In this study, we found that, compared with the Control group, expression of Bcl-XL and Bcl-2 proteins in the Model groups was significantly downregulated in a time-dependent manner. Compared with the Control group, expression Bax and Bak proteins in the Model groups was remarkably upregulated in a time-dependent manner. Moreover, levels of cleaved caspase 3, which is an active form of caspase 3 [31], were significantly higher in the Model-8 h, Model-12 h, and Model-24 h groups than in the Control group. Therefore, the LPS administration caused the activated caspase 3 mediated apoptosis in the lung tissues of ALI mice. All of the above results suggest that LPS administration significantly induces apoptosis through activating the mitochondria-mediated signaling pathway. These findings remind us that the mitochondria-mediated apoptosis should be considered carefully when investigating the role of molecules in LPS-induced animal models. However, our study did not determine the specific mechanism underlying the LPS-induced apoptotic pathway by evaluating activities of the other caspases and cytochrome C levels in lung tissues, all of which could further strengthen our findings.

RanBPM is a nucleo-cytoplasmic and evolutionarily conserved molecule that participates in many intra-cellular pathways via modulating various cellular functions [32] such as apoptosis, cell migration, cell adhesion, and transcription [33]. A previous study [34] also reported that RanBPM could mimic or potentiate amyloid  $\beta$  ( $A\beta$ ) to induce mitochondrial dysfunction, and finally cause neurodegenerative progress in Alzheimer's disease. In our LPS-induced ALI model, RanBPM demonstrated the same apoptosis-promoting effect in lung injury cells, which is consistent with the change in Bax and Bak expression. Therefore, RanBPM may participate in the Bcl-2 family-mediated mitochondrial apoptosis pathway. However, this study only investigated the changes in related protein expression, and could not clarify the specific role of RanBPM in the mitochondria-mediated apoptosis pathway. Moreover, the targeting cells for RanBPM have not been identified in this study, which is a limitation.

## Conclusions

LPS administration causes obvious inflammatory cell infiltration, increased W/D ratio, and MPO activity. Meanwhile,

LPS administration decreased Bcl-XL and Bcl-2 expression, increased Bak and Bax expression, enhanced RanBPM expression, and upregulated cleaved caspase 3 expression in lung tissues in the ALI mouse model groups. In summary, lipopolysaccharide-induced acute lung injury is associated with increased RanBPM molecule expression and with the mitochondria-mediated apoptosis signaling pathway in a mouse model.

## Conflict of interest

None.

## References:

- Li S, Cui HZ, Xu CM et al: RUNX3 protects against acute lung injury by inhibiting the JAK/STAT3 pathway in rats with severe acute pancreatitis. *Eur Rev Med Pharmacol Sci*, 2019; 23: 5382–91
- Qu L, Chen C, Chen Y et al: High-mobility group Box 1 (HMGB1) and autophagy in acute lung injury (ALI): A review. *Med Sci Monit*, 2019; 25: 1828–37
- Toki S, Zhou W, Goleniewska K et al: Endogenous PGI<sub>2</sub> signaling through IP inhibits neutrophilic lung inflammation in LPS-induced acute lung injury mice model. *Prostaglandins Other Lipid Mediat*, 2018; 136: 33–43
- Malhotra A: Low-tidal-volume ventilation in the acute respiratory distress syndrome. *N Engl J Med*, 2007; 357: 1113–20
- Matthay MA, Ware LB, Zimmerman GA: The acute respiratory distress syndrome. *J Clin Invest*, 2012; 122: 2731–40
- Rebetz J, Semple JW, Kapur R: The pathogenic involvement of neutrophils in acute respiratory distress syndrome and transfusion-related acute lung injury. *Transfus Med Hemother*, 2018; 45: 290–98
- Semple JW, Rebetz J, Kapur R: Transfusion-associated circulatory overload and transfusion-related acute lung injury. *Blood*, 2019; 133: 1840–53
- Kapur R, Kim M, Rebetz J et al: Gastrointestinal microbiota contributes to the development of murine transfusion-related acute lung injury. *Blood Adv*, 2018; 2: 1651–63
- Kapur R, Kasetty G, Rebetz J et al: Osteopontin mediates murine transfusion-related acute lung injury via stimulation of pulmonary neutrophil accumulation. *Blood*, 2019; 134: 74–84
- Wheeler AP, Bernard GR: Acute lung injury and the acute respiratory distress syndrome: A clinical review. *Lancet*, 2007; 369: 1553–64
- Zhang B, Wang B, Cao S et al: Silybin attenuates LPS-induced lung injury in mice by inhibiting NF- $\kappa$ B signaling and NLRP3 activation. *Int J Mol Med*, 2017; 39: 1111–18
- Zhou J, Zhou Z, Ji P et al: Effect of fecal microbiota transplantation on experimental colitis in mice. *Exp Ther Med*, 2019; 17: 2581–86
- Zhang Y, Tian K, Wang Y et al: The effects of aquaporin-1 in pulmonary edema induced by fat embolism syndrome. *Int J Mol Sci*, 2016; 17: E1183
- Kong G, Huang X, Wang L et al: Astilbin alleviates LPS-induced ARDS by suppressing MAPK signaling pathway and protecting pulmonary endothelial glycocalyx. *Int Immunopharmacol*, 2016; 36: 51–58
- Liu H, Hao J, Wu C et al: Eupatilin alleviates lipopolysaccharide-induced acute lung injury by inhibiting inflammation and oxidative stress. *Med Sci Monit*, 2019; 25: 8289–96
- Johnson ER, Matthay MA: Acute lung injury: Epidemiology, pathogenesis, and treatment. *J Aerosol Med Pulm Drug Deliv*, 2010; 23: 243–52
- Fu C, Dai X, Yang Y et al: Dexmedetomidine attenuates lipopolysaccharide-induced acute lung injury by inhibiting oxidative stress, mitochondrial dysfunction and apoptosis in rats. *Mol Med Rep*, 2017; 15: 131–38
- O'Neill KL, Huang K, Zhang J et al: Inactivation of pro-survival Bcl-2 proteins activates Bax/Bak through the outer mitochondrial membrane. *Gene Dev*, 2016; 30: 973–88
- Gong X, Ye W, Zhou H et al: RanBPM is an acetylcholinesterase-interacting protein that translocates into the nucleus during apoptosis. *Acta Biochim Biophys Sin (Shanghai)*, 2009; 41: 883–91
- Dong ZW, Yuan YF: Juglanin suppresses fibrosis and inflammation response caused by LPS in acute lung injury. *Int J Mol Med*, 2018; 41: 3353–65
- Gao P, Zhao Z, Zhang C et al: The therapeutic effects of traditional Chinese medicine fusu agent in LPS-induced acute lung injury model rats. *Drug Des Devel Ther*, 2018; 12: 3867–78
- Park JR, Lee H, Kim SI et al: The tri-peptide GHK-Cu complex ameliorates lipopolysaccharide-induced acute lung injury in mice. *Oncotarget*, 2016; 7: 58405–17
- Matute-Bello G, Downey G, Moore BB et al: An official American thoracic society workshop report: features and measurements of experimental acute lung injury in animals. *Am J Respir Cell Mol Biol*, 2011; 44: 725–38
- Hughes KT, Beasley MB: Pulmonary manifestations of acute lung injury: More than just diffuse alveolar damage. *Arch Pathol Lab Med*, 2017; 141: 916–22
- Meng L, Zhao X, Zhang H: HIPK1 interference attenuates inflammation and oxidative stress of acute lung injury via autophagy. *Med Sci Monit*, 2019; 25: 827–35
- Fragoso IT, Ribeiro EL, Gomes FO et al: Diethylcarbamazine attenuates LPS-induced acute lung injury in mice by apoptosis of inflammatory cells. *Pharmacol Rep*, 2017; 69: 81–89
- Fahmi ANA, Shehatou GSG, Salem HA: Levocetirizine pretreatment mitigates lipopolysaccharide-induced inflammation in rats. *Biomed Res Int*, 2018; 2018: 7019759
- Zhang WW, Geng X, Zhang WQ: Downregulation of lncRNA MEG3 attenuates high glucose-induced cardiomyocytes injury by inhibiting mitochondrial-mediated apoptosis pathway. *Eur Rev Med Pharmacol Sci*, 2019; 23: 7599–604
- Um HD: Bcl-2 family proteins as regulators of cancer cell invasion and metastasis: A review focusing on mitochondrial respiration and reactive oxygen species. *Oncotarget*, 2016; 7: 5193–203
- Lan T, Zhao H, Xiang B et al: Suture compression induced midpalatal suture chondrocyte apoptosis with increased caspase-3, caspase-9, Bax, Bak and Bid expression. *Biochem Biophys Res Commun*, 2017; 489: 179–86
- Crowley LC, Waterhouse NJ: Detecting cleaved caspase-3 in apoptotic cells by flow cytometry. *Cold Spring Harb Protoc*, 2016; 2016: 087312
- Das S, Hag S, Ramakrishna S: Scaffolding protein RanBPM and its interactions in diverse signaling pathways in health and disease. *Discov Med*, 2018; 25: 177–94
- Salemi LM, Maitland MER, McTavish CJ et al: Cell signaling pathway regulation by RanBPM: Molecular insights and disease implications. *Open Biol*, 2017; 7: 170081
- Roh SE, Woo JA, Lakshmana MK et al: Mitochondrial dysfunction and calcium deregulation by the RanBPM9-cofilin pathway. *FASEB J*, 2013; 27: 4776–89